https://doi.org/10.5194/egusphere-2024-1621
Preprint. Discussion started: 27 June 2024

Technical note: Refining $\delta^{15}N$ isotopic fingerprints of local NOx for accurate source identification of nitrate in $PM_{2.5}$

Hao Xiao [1,2], Qinkai Li [3], Shiyuan Ding [2], Wenjing Dai [2], Gaoyang Cui [4], Xiaodong Li [2*]

[1] School of Agriculture and Biology, Shanghai Jiao Tong University, Shanghai, 200240, China;

[2] Institute of Surface-Earth System Science, School of Earth System Science, Tianjin University, Tianjin, 300072, China;

[3] Jiangxi Key Laboratory of Environmental Pollution Control, Jiangxi Academy of Eco-Environmental Sciences and Planning, Nanchang, 330039, China;

[4] The College of Geography and Environmental Science, Henan University, Kaifeng, 475004, China;

* Correspondence: Xiaodong Li (xiaodong.li@tju.edu.cn)

Abstract

Stable nitrogen isotopic composition ($\delta^{15}N$) has proven to be a valuable tool for identifying sources of nitrates (NO_3^-) in $PM_{2.5}$. However, the absence of a systematic study on the $\delta^{15}N$ values of domestic NOx sources hinders accurate identification of NO_3^- sources in China. Here, we systematically determined and refined $\delta^{15}N$ values for six categories of NOx sources in the local Tianjin area using an active sampling method. Moreover, the $\delta^{15}N$ values of NO_3^- in $PM_{2.5}$ were measured during pre-heating, mid-heating and late-heating periods, which are the most heavily polluted in Tianjin. Results shown that the representative nature and region-specific characteristics of isotopic fingerprints for six categories of NOx sources in Tianjin. The Bayesian isotope mixing (MixSIAR) model demonstrated that coal combustion, biomass burning, and vehicle exhaust collectively contributed more than 60%, dominating the sources of NO_3^- during sampling periods in Tianjin. However, failure to consider the isotopic signatures of local NOx sources could result in an underestimation of the contribution from coal combustion. Additionally, the absence of industrial sources, an uncharacterized source in previous studies, may directly result in the contribution fraction of other sources being overestimated by the model more than 15%. Notably, as the number of sources input to the model increased, the contribution of various NOx sources was becoming more stable, and the inter-influence between various sources significantly reduced. This study demonstrated that the refined isotopic fingerprint in a region-specific context could more effectively distinguish source of NO_3^-, thereby providing valuable insights for controlling NO_3^- pollution.

1. Introduction

In recent decades, the acceleration of urbanization and modernization in China

https://doi.org/10.5194/egusphere-2024-1621
Preprint. Discussion started: 27 June 2024

has inevitably led to persistent and frequent incidents of atmospheric $PM_{2.5}$ pollution in urban areas (Zhang et al., 2023;Meng et al., 2024). SNA (SO_4^{2-}, NO_3^- and NH_4^+) constitutes one of the most important components of $PM_{2.5}$, and its elevated concentration will exacerbate the pollution level of $PM_{2.5}$ (Huang et al., 2014). A series of scientific and effective air pollutant emission control measures has led to a significant decrease in the concentration of SO_4^{2-} in $PM_{2.5}$ in urban areas of China has decreased significantly (Wang et al., 2022). However, the concentration and percentage of NO_3^-in $PM_{2.5}$ have shown a gradual increase (Wang et al., 2022;Zhang et al., 2020). Previous studies have indicated that NO_3^- has surpassed SO_4^{2-} as the primary inorganic component of atmospheric $PM_{2.5}$ in the northern Chinese cities, with mass concentrations accounting for approximately 5% ~ 26% (Zong et al., 2022b;Zhang et al., 2019;Xie et al., 2019). Consequently, the accurate identification of the sources of NO_3^- is essential for the development of effective air management measures, which can effectively control the occurrence of urban haze weather.

The accurate identification of the sources of atmospheric NOx was complicated by the considerable complexity and diversity of the sources involved, which include, but are not limited to, coal combustion, vehicle exhaust, biomass burning and soil emissions (Huang et al., 2017;Duncan et al., 2016). The reliable identification of the sources of NOx in the atmosphere was achieved using stable nitrogen isotopes composition ($\delta^{15}N$) (Zong et al., 2017;Song et al., 2021). However, to achieve the most accurate results, it is essential to accurately identify the $\delta^{15}N$ values of the atmospheric NOx source (Zhang et al., 2024a;Lin et al., 2021). Although the $\delta^{15}N$ values from some NOx sources have been reported by other studies (Zong et al., 2020a;Zong et al., 2022a). However, the majority of current research reports on the $\delta^{15}N$ values of NOx from different sources in the atmosphere originates from foreign countries, and the collection methods have not been unified (Elliott et al., 2019;Walters et al., 2015a;Walters et al., 2015b). For instance, Felix and Elliott (2014) reported the $\delta^{15}N$-NOx from vehicle exhaust as +14.2 ± 1.9‰ based on the active sampler. However, a relatedly negative value (−11.4 ± 6.9‰) from vehicle exhaust was reported by the passive sampler (Walters et al., 2018). Similar discrepancies have also been observed in other NOx sources (Li and Wang, 2008;Elliott et al., 2019). Furthermore, the production mechanisms of different NOx types can also affect its $\delta^{15}N$ values, such as fuel type NOx and thermal type NOx (Heaton, 1990). Coal combustion can result in the release of both fuel type NOx and thermal type NOx, due to the high combustion temperature and the abundant nitrogen components (Heaton, 1990;Felix et al., 2012). However, biomass burns at low temperatures (250 to 1200 °C), and the process produces mainly fuel NOx, with $\delta^{15}N$ depending on the relative abundance of nitrogenous organic matter ^{15}N in the biomass itself (Zong et al., 2022a). Therefore, considering the regional differences in the relative abundance of ^{15}N in fuels (Zong et al., 2022a;Shi et al., 2022), these $\delta^{15}N$ values reported abroad for fuel-based NOx may not be applicable to domestic studies. Furthermore, the previous studies have not yet provided a comprehensive overview of the $\delta^{15}N$ values of NOx sources. There is a lack of systematic studies on the $\delta^{15}N$ characteristics of different NOx sources at both the domestic and international level. For instance, the $\delta^{15}N$

https://doi.org/10.5194/egusphere-2024-1621
Preprint. Discussion started: 27 June 2024

values of NOx from industrial emissions and natural gas combustion in urban areas have rarely reported. Despite these sources being included in the NOx emission inventory, the current isotopic fingerprint database lacks a clear definition. In this context, the use of associated model calculations to quantify the source contribution of NOx or NO_3^- to the regional atmosphere may introduce a high level of uncertainty (Zhang et al., 2024a). Therefore, it is of great significance to enhance the existing $\delta^{15}N$ values of NOx sources.

Tianjin, recognized as one of most heavily polluted cities in China, experiences strongly influenced from severe haze pollution (Xiao et al., 2022, 2023;Xiao et al., 2024b). Particularly during heating periods, episodes of haze formation characterized by abrupt increases in NO_3^- concentrations have been observed (Zou et al., 2018;Feng et al., 2020). This phenomenon is attributable to the predominant use of coal as the primary heating fuel in Tianjin, resulting in considerable NOx emissions (Zhao et al., 2021). Recent research efforts in Tianjin have focused on identifying the sources of NO_3^- through its dual isotopic compositions (Zhang et al., 2019;Xiao et al., 2023). Nevertheless, there is a paucity of systematic characterization of the $\delta^{15}N$-NOx source signatures in Tianjin, and even in China, which contributes to significant uncertainties regarding NOx source contributions (Zhang et al., 2024a). Consequently, to enhance understanding of atmospheric NO_3^- sources, it is imperative to refine the $\delta^{15}N$ values of various local sources in Tianjin.

Here, we established a refined isotopic fingerprint for major NOx sources in Tianjin area using an active sampling method, which including previously uncharacterized sources in China such as industrial emissions and natural gas combustion. To better understand the need for established refined isotopic fingerprint in a region-specific context for major NOx sources, $PM_{2.5}$ samples were collected in Tianjin across three distinct periods: pre-heating (29th October 2018 to 25th November 2018), mid-heating (8th January 2019 to 22nd January 2019), and late-heating (7th March 2019 to 3rd April 2019). Based on the Bayesian isotope mixing (MixSIAR) model, this study compares and explains the differences in the source resolution results due to the $\delta^{15}N$-NOx sources measured locally in Tianjin and those measured by previous studies. Notably, coal combustion activity was most pronounced during the mid-heating period compared to other periods. Given the proposition that coal combustion is a significant source of NO_3^-, it is conceivable that coal combustion would exhibit a notably higher contribution fraction during the mid-heating period compared to the pre-heating and late-heating periods (Feng et al., 2020). This provides an opportunity to explore the necessity of establishing local source $\delta^{15}N$ values for NOx emissions in Tianjin. The study will enhance our understanding of the source of NO_3^- in $PM_{2.5}$, and further emphasize the necessity for the establishment of a refined isotopic fingerprint for NOx sources in future studies.

https://doi.org/10.5194/egusphere-2024-1621
Preprint. Discussion started: 27 June 2024

2. Materials and Methods

2.1 Description of the location and sample collection

$PM_{2.5}$ samples were collected from the rooftop of Tianjin University, located in the Nankai District, Tianjin (Figure S1). The roof stands approximately 25 m above ground level, with no discernible sources of pollutants in the vicinity, such as factories or construction sites. A high-volume air sampler (Tisch, USA) equipped with quartz fiber filters (Pallflex, 20 × 25 cm) was utilised for $PM_{2.5}$ collection, operating at a flow rate of 1.05 m^3 min^{-1}. Prior to sampling, all quartz fiber filters underwent combustion at 450°C for 6 hours to eliminate potential interference from organic matter. Samples were collected at two distinct time points: daytime samples between 8:00 and 18:00, and nighttime samples between 18:30 and 7:30 the following morning. Pollutant concentrations (e.g., $PM_{2.5}$, SO_2, NO_2, CO) and corresponding meteorological parameters (e.g., ambient temperature, T; relative humidity, RH; wind speed, WS) during sampling periods were obtained from nearby monitoring stations (Xiao et al., 2024b).

To enable comparison, a diaphragm pump (Laoying 3072, Qingdao Laoying Environmental Science and Technology, China) was uniformly employed to actively absorb NOx emissions from various sources (Figure S2). Initially, hydrophobic Teflon membrane (TF-200, Pall, USA) and nylon membrane (BNRG810S, Pall, USA) were used to exclude interference of particulate NO_3^- and gaseous HNO_3 emitted by sources, respectively. Filtered gases were then passed through an alkaline solution of 0.5 mol L^{-1} NaOH and 0.25 $KMnO_4$, known for its strong oxidizing properties, oxidizing NOx entering the absorbing solution to form NO_2^- or NO_3^- and store it in the absorbing vial (Fibiger et al., 2014;Fibiger and Hastings, 2016). The added NaOH served to react with NOx and enhance the viscosity of the absorbing solution, thereby improving conversion efficiency (Sada et al., 1977). However, since $KMnO_4$ in the absorbing solution is in excess, incompletely reacted $KMnO_4$ in the solution must be further reduced in the laboratory. This study involved 6 emission sources of NOx in the local Tianjin area, including coal-fired power plants, gas-fired power plants, biomass burning, vehicle exhaust, iron and steel smelting and soil emission sources (see Supporting Information Text S1 for detailed description). All collected $PM_{2.5}$ samples and gaseous NOx from various sources were stored at -20 °C in a refrigerator after sampling. It was worth noting that an additional blank sample was prepared for each sampling campaign, in parallel with the other samples.

2.2 Chemical and isotopic analysis

In the ultraclean room, a proportion of the particulate matter from the each $PM_{2.5}$ sample was cutted and transferred to a 50 ml centrifuge tube. Subsequently, samples from each filter were extracted using Milli-Q water, which has a demonstrated ionic strength of 18.2 MΩ cm (Millipore, United States), via ultrasonication and

https://doi.org/10.5194/egusphere-2024-1621
Preprint. Discussion started: 27 June 2024

centrifugation. Ionic chromatography (Dionex Aquion, Thermo Fisher Scientific, Inc., Waltham, MA, USA) was employed following established methodologies to determine the presence of water-soluble major ions (e.g., SO_4^{2-}, NO_3^-, and NH_4^+) in $PM_{2.5}$ (Xiao et al., 2024b). For the gaseous NOx samples from various sources, an excess of H_2O_2 was added to the absorbent solution until all the incompletely reacted $KMnO_4$ in the sampled absorbent solution was converted, resulting in the formation of black MnO_2 precipitate (Fibiger and Hastings, 2016). Subsequently, the resulting suspension was centrifuged at high speed (4000 r min^{-1}) for 10 minutes to obtain the supernatant, which was neutralized using electronic grade hydrochloric acid (HCl) at a mass concentration of approximately 38% to neutralize under-reacted sodium hydroxide. Finally, the supernatant was analyzed for NO_2^- and NO_3^- concentrations on a Skalar San++ continuous flow nutrient salt analyzer. It was noteworthy that the concentration of NO_2^- in the absorbent solution after treatment with a strong oxidant (i.e., H_2O_2) as described above is typically extremely low, typically below 0.005 μg mL^{-1}.

In this study, we utilized the bacterial denitrification method to determine the dual isotopic values of NO_3^- ($\delta^{15}N$ and $\delta^{18}O$) in $PM_{2.5}$ and absorbent solution. Further details can be found in our previous study (Xiao et al., 2023;Li et al., 2021). Briefly, extracted NO_3^- were quantitatively converted to N_2O through the action of denitrifying bacteria, namely Pseudomonas aureofaciens, ATCC 13985, which lacked N_2O reductase (Luo et al., 2020b). Subsequently, the $\delta^{15}N$ and $\delta^{18}O$ values of N_2O were determined using GasBench-II with continuous flow isotope ratio mass spectrometry (IRMS; Thermo Fisher DELTA V advantage, Thermo Fisher Scientific, Inc.) for on-line analysis. The study employed three isotopic international standards: USGS32, USGS34 and IAEA-N3, and the analytical accuracies for both $\delta^{15}N$ and $\delta^{18}O$ were ± 0.2‰ and ± 0.3‰, respectively. Furthermore, the influence of NO_2^- was deemed negligible as its concentration fell below 2% of the NO_3^- level in all samples (Luo et al., 2019).

2.3 Stable isotopic mixing model

The Bayesian model enabled the determination of the probability distribution of the contribution of each source to a mixture (Parnell et al., 2010). Subsequently, a Bayesian isotope mixing model was implemented in the R software package (Stable Isotope Analysis in R, SIAR) to estimate potential sources of atmospheric NO_3^- in $PM_{2.5}$ in this study (Zong et al., 2017). Briefly, the model initiates with establishing a logistic prior distribution, followed by determining the probability contribution distribution of each source to the mixture. Further details are available in our previous study (Xiao et al., 2023;Li et al., 2021). It was noteworthy that an obvious isotopic fractionation process occurs during the conversion of NOx to NO_3^-. Therefore, the nitrogen isotope fractionation coefficient (εN) resulting from NOx to NO_3^- conversion should be calculated prior to determining the relative contribution of NOx sources using MixSIAR model (Text S2). Furthermore, to enhance the reliability of the study results, the model generated 10,000 potential scenarios for each evaluated potential

https://doi.org/10.5194/egusphere-2024-1621
Preprint. Discussion started: 27 June 2024

source (Song et al., 2019;Fan et al., 2020).

3. Results and discussion

3.1 The $\delta^{15}N$ values of major NO_x emission sources

This study sampled three categories of NO_x sources associated with the combustion of fossil fuels, specifically vehicle exhaust, coal combustion, and natural gas combustion. As shown in Figure 1 and Table 1, the NOx concentrations emitted by these sources exceeded atmospheric NOx concentration levels in urban China. The $\delta^{15}N$ values and concentrations of NOx in vehicle exhaust exhibited a range of −18.3 ‰ to 7.9 ‰ and 0.006 to 223.8 ppm, respectively. Furthermore, slight differences were observed between the $\delta^{15}N$ values in vehicle exhaust at different sampling sites (Figure S3), which can be attributed to the varying nitrogen contents of the fuels, the NOx generation pathways and the efficiency of the three-way catalytic devices (Walters et al., 2015a;Zong et al., 2020a;Heaton, 1990). For instance, vehicle exhaust can produce both thermal and fuel NOx. Thermal NOx is generated at high temperatures exceeding 1500°C and is influenced by factors such as the molar concentrations of O_2 and N_2 and combustion temperature (Walters et al., 2015b). In contrast, fuel NOx is primarily related to the nitrogen content of the fuel (Walters et al., 2015b). Walters et al. (2015a) observed that fuel NOx exhibited more positive $\delta^{15}N$ values than thermal NOx, and catalytic treatment could also yield positive $\delta^{15}N$ values. When compared with previous studies (Figure S4a and Table 1), our results align with domestic reports but significantly differ from foreign studies. This variation can be attributed to significant differences in $\delta^{15}N$ values of oils due to their generation and depositional settings (Williams et al., 1995), indicating local characteristics of $\delta^{15}N$ values of NOx in vehicle exhaust.

The $\delta^{15}N$ value of NOx emissions from the coal-fired power plant (coal combustion) in Tianjin ranged from +9.4 ‰ to +15.4 ‰, with a mean value of +12.3 ± 1.7 ‰ (Figure 1). Our results differ significantly from previous reported $\delta^{15}N$-NOx values from coal combustion (Figure S4b). A previous study found that the $\delta^{15}N$-NOx values from coal combustion were primarily influenced by thermal NOx production related to combustion temperature and NOx reduction technology related to fuel-to-air ratio, rather than by $\delta^{15}N$ values of the coal itself (Felix et al., 2012). However, the coal combustion temperatures of approximately 1300 to 1400 °C observed in power plants in this study were insufficient to produce thermal NOx (Heaton, 1990). Consequently, the $\delta^{15}N$-NOx value from coal combustion in this study may be related to the ^{15}N abundance of coal, indicating local characteristics of $\delta^{15}N$ values of NOx from coal combustion. It is noteworthy that a considerable range of values (-31.3 ‰ ~ -17.5 ‰) and a relatively negative mean value (-24.8 ± 5.6 ‰) of $\delta^{15}N$-NOx from natural gas combustion were observed, in comparison to the aforementioned sources (Figure 1). Generally, natural gas has a low nitrogen content, and its combustion primarily produces thermal NOx, with $\delta^{15}N$ values depending on temperature, pressure and oxygen content in the combustion chamber (Heaton, 1990). In this study, the combustion chamber of a gas-fired power plant can have a temperature of more

https://doi.org/10.5194/egusphere-2024-1621
Preprint. Discussion started: 27 June 2024

than 2000 °C, generating NOx mainly through the extended Zeldovich mechanism (Zong et al., 2020a). Consequently, the $\delta^{15}N$ values of NOx from natural gas combustion exhibit a significantly more negative trend than those observed in the two aforementioned sources. However, our results were more negative than those reported by Walters et al. (2015b) for NOx emitted from residential gas furnaces in Indiana, USA (ranging from -19.7 ‰ to -13.9 ‰ and -16.5 ± 1.7 ‰). This discrepancy can be attributed to the combustion process employed in this study, which necessitates the introduction of sufficient air into the combustion chamber. To achieve this, 'fresh air' was introduced into to the chamber, which may have resulted in a reduction in $^{14}N^{14}N$ loss and the generation of negative $\delta^{15}N$-NOx values in this study compared to those observed in previous studies.

NOx emissions from industrial sources, such as the iron and steel industry, arise from various processes including sintering, pelletizing, and hot blast furnaces (Wang et al., 2019;Zhao et al., 2017). Generally, the $\delta^{15}N$-NOx value from industrial emission sources differs significantly from those of emissions from fossil fuel combustion (Figure 1b), emphasizing the representativeness of the isotopic fingerprint in industrial emission sources. The $\delta^{15}N$ values of NOx emitted from the hot blast furnace were −43.1 ± 12.3 ‰, in contrast to the more positive value observed for the sintering process (−14.5 ± 3.2‰) and the pelletizing process (−6.4 ± 2.5‰) (Figure S5). This suggests that the mechanisms by which these processes emit NOx were complex and highly variable. The maximum temperature in the central area of the hot air stove can exceed 2000 °C, with the majority of emitted NOx being thermal NOx (Toof, 1986). Due to the continuous $^{14}N^{14}N$ supplementation, generated NOx exhibits a negative $\delta^{15}N$. In contrast, the temperatures of sintering and pelletizing processes are relatively low (1200 ~ 1400 °C), with the majority of emitted NOx being fuel-type NOx (Toof, 1986). Specifically, functional groups such as pyrrole and pyridine in coke powder decompose at high temperatures and react with O_2 to produce NO_x, resulting in a positive value of $\delta^{15}N$-NOx (Hayhurst and Vince, 1980). It should be noted that the raw materials used for sintering were iron ore fines and coke powder, which differed from those used in coal combustion in power plants. Consequently, the $\delta^{15}N$ values of NOx released cannot be considered to be the same source isotopic fingerprint, as they are influenced by differences in ^{15}N abundance (Heaton, 1990).

This study also characterizes $\delta^{15}N$-NOx values released from biomass burning (+1.2 ± 3.0 ‰), obtained by burning various types of plant materials locally in Tianjin. The mean values observed in this study were comparable to those reported by Fibiger and Hastings (2016) (+1.0 ± 4.1 ‰), while the range of fluctuations (−4.9 ‰ ~ +5.5 ‰) was narrower than those observed by their results (−7 ‰ ~ +12 ‰) (Figure S4d). Moreover, the $\delta^{15}N$ values of biomass fuel combustion from the Zhejiang Province, China, which measured the $\delta^{15}N$-NOx values of biomass burning from various types of biomass fuels [Shi et al., 2022], were found to be lower than those observed in the present study. These results indicate that the variations in the $\delta^{15}N$-NOx values of biomass burning are primarily influenced by the type of biomass fuel (Shi et al., 2022). Similarly, significant differences were observed between various

https://doi.org/10.5194/egusphere-2024-1621
Preprint. Discussion started: 27 June 2024

types of biomass fuel combustion, supporting this viewpoint (Figure S6). These findings indicate that the NOx from biomass burning worldwide may exhibit a wide range of $\delta^{15}N$ values due to varying $\delta^{15}N$-biomass values. Consequently, in order to accurately assess the contribution of biomass burning to atmospheric NOx in Tianjin, it is essential to obtain the ^{15}N signal of NOx release from typical local biomass combustion is essential.

In comparison to the five sources mentioned earlier, soil emission exhibits a lower concentration of NOx, accompanied by the most negative $\delta^{15}N$ value (-33.7 ± 9.7 ‰) (Figure 1). Moreover, the concentration or $\delta^{15}N$ values of NOx released from various types of soil demonstrate a clear distinction (Figure S7). The concentration of NOx released from wheatland soil after irrigation was found to be significantly higher than that observed prior to irrigation (Figure S7). However, the difference in $\delta^{15}N$ of NOx (-38.5 ± 2.5 ‰ vs. -40.1 ± 5.9 ‰) was not found to be significant ($p > 0.05$). These results indicate that irrigation has a significantly impact on NOx release from wheatland soils, but not on its $\delta^{15}N$ value. The $\delta^{15}N$-NOx released from wetland soils was comparable to that released from wheatland soils, both of which exhibited a more negative value than those released from urban green belt soils (Figure S7). Previous studies have indicated that soil NO release is primarily divided into biotic and abiotic processes (Hall et al., 1996). The biotic process encompasses the nitrification of NH_4^+ and the denitrification of NO_3^-, while the abiotic process is primarily the chemical reduction of NO_2^- in soil (Yu and Elliott, 2017). Kinetic processes favor the presence of ^{14}N in the product gases derived from the biotic process, whereas the $\delta^{15}N$-NOx released by abiotic processes in soil is significantly positive than that of biotic processes (Felix and Elliott, 2014;Li and Wang, 2008;Baggs, 2008). Consequently, our study suggests that a significant abiotic process may have caused NO release from urban green belt soils. Given the abundance of wheatland in the vicinity of Tianjin and the urban area covered by green belts and coastal wetlands, we used the aforementioned $\delta^{15}N$-NOx values from the three soil types as representative of local soil emissions in Tianjin.

3.2 Characteristics of concentration and $\delta^{15}N$ value of NO_3^- in $PM_{2.5}$

3.2.1 Concentrations of $PM_{2.5}$ and NO_3^-

The $PM_{2.5}$ concentration ranged from 5.1 μg m^{-3} to 297.8 μg m^{-3} during the sampling period in Tianjin, with an average value of 68.6 ± 62.4 μg m^{-3} (Table 2 and Figure 2). Pre-heating exhibited the highest mean concentration (75.3 ± 53.3 μg m^{-3}), followed by mid-heating (68.9 ± 43.2 μg m^{-3}) and late-heating (39.0 ± 27.9 μg m^{-3}). SNA (Sulfate: SO_4^{2-}, Nitrate: NO_3^-, Ammonium: NH_4^+) constituted the major ions in $PM_{2.5}$, contributing to over 40% of $PM_{2.5}$ (Figure S8). The concentration of NO_3^- showed a significant positive linear correlation with $PM_{2.5}$ (Figure 2), suggesting that the substantial increase in $PM_{2.5}$ pollution is linked to an increase in NO_3^- concentration.

The variation pattern of NO_3^- concentration during different sampling periods aligned with that of $PM_{2.5}$ (Figure 2). The highest concentration of NO_3^- was

https://doi.org/10.5194/egusphere-2024-1621
Preprint. Discussion started: 27 June 2024

observed during pre-heating (16.0 ± 12.4 μg m^{-3}), and the lowest concentration was observed during late-heating (9.7 ± 8.7 μg m^{-3}) (Table 2). Notably, NO_2, as the precursor of NO_3^-, did not follow the observed pattern of change in NO_3^- concentration. The highest concentration of NO_2 was observed during mid-heating (Table S1 and Figure S7), potentially influenced by increased coal combustion for heating (Luo et al., 2019). Generally, NO_2 concentration and its secondary conversion efficiency were the key factors affecting the concentration of NO_3^-. Therefore, the difference could be attributed to biases in the secondary conversion efficiency of NO_2 (Xiao et al., 2023). This is supported by the lower relative humidity (RH) during mid-heating (31.1 ± 20.3%) compared to pre-heating (46.2 ± 14.8%) (Table S1), as higher RH could lead to increased NO_3^- formation (Gao et al., 2020). Compared to NO_3^-, the SO_4^{2-} concentration was highest during mid-heating. In addition, SO_2, mainly originating from coal combustion, exhibited a similar variation pattern to SO_4^{2-}, potentially attributed to increased coal combustion for heating (Figure S9) (Feng et al., 2020). Markers primarily originating from coal combustion, including CO and Cl^- (Figure S9), also showed higher concentration during mid-heating, supporting our speculation (Luo et al., 2019;Xiao et al., 2022). While the increase in NO_2 could be attributed to enhanced biomass burning during mid-heating, the concentration of K^+, primarily a biomass burning marker (Xiao et al., 2024a), exhibited slight variation during the three periods and was significantly lower than Cl^- (Table 2). Thus, the impact of coal combustion heating on NO_3^- sources was evident, despite mid-heating periods being unfavorable for NO_3^- generation.

3.2.2 Characteristics in $\delta^{15}N$ value of NO_3^-

The $\delta^{15}N$-NO_3^- values in this study ranged from -0.7‰ to 20.8‰, with a mean $\delta^{15}N$ value of 8.5 ± 4.4‰ (Figure 2 and Table 2). This measurement was more negative than the observations reported by Feng et al. (2020) (14.1 ± 3.2‰) in Tianjin in 2017, Luo et al. (2019) in Beijing (13.9 ± 2.4‰) in 2013, and Zhang et al. (2021) in Beijing (+11.5 ± 5.0‰) in 2018. The Coal Replacement Project, initiated since 2017 to replace coal with cleaner energy sources such as natural gas and electricity in major cities such as Beijing and Tianjin in northern China (Feng et al., 2020), could explain this reduction in coal use leading to a gradual decrease in $\delta^{15}N$ values of NO_3^-, as NOx emissions from coal combustion have positive $\delta^{15}N$ values. This speculation is supported by reported changes in the Bohai Sea from 2014 to 2019 (Zong et al., 2022b).

Significant differences were observed in $\delta^{15}N$-NO_3^- values among the three sampling periods in this study. The most positive value was observed during mid-heating (12.4 ± 3.3‰), followed by pre-heating (7.7 ± 4.1‰) and late-heating (7.1 ± 4.1‰) (Table 2). These results suggest variations in the sources of NOx during three sampling periods. For instance, the primary source $\delta^{15}N$-NOx from coal combustion (+12.3 ± 1.7 ‰) has most positive value (Figure 1), indicating coal combustion as the dominant source of NOx during mid-heating periods (Luo et al., 2019). However, for the other sampling periods, the $\delta^{15}N$ values of NO_3^- indicate multiple sources of NOx, including fossil fuel combustion, industrial emissions, biomass burning, and soil

https://doi.org/10.5194/egusphere-2024-1621
Preprint. Discussion started: 27 June 2024

sources (Zong et al., 2017;Sun et al., 2020). Previous studies conducted in Chinese cities have reported monthly variations in $\delta^{15}N\text{-}NO_3^-$, which could also be attributed to changing NOx sources (Luo et al., 2020a;Luo et al., 2020b;Guo et al., 2021;Zhang et al., 2022).

3.3 The importance of $\delta^{15}N$ values from local NOx source for sources apportionment of NO_3^- in $PM_{2.5}$

In this study, the MixSIAR model was employed to quantify the contribution of NOx sources. Previous studies have estimated the contribution of NOx sources using the MixSIAR model, based on the known $\delta^{15}N$ values of NOx from different sources. These studies have focused on four sources of NOx: coal combustion, biomass combustion, vehicle exhaust, and soil sources (Zong et al., 2017;Zong et al., 2020b;Zhao et al., 2020;Zhang et al., 2020). To facilitate comparison, the $\delta^{15}N$ data of above four sources from previous studies (Scenario 1) and this study (Scenario 2) were input into the MixSIAR model to quantify the sources of NO_3^-, respectively (Table 1). Throughout the entire sampling duration, the average contributions estimated by the MixSIAR model exhibited no substantial disparities between Scenarios 1 and 2, suggesting that localized $\delta^{15}N$ data acquisition for NOx sources might be superfluous. However, the contributions of individual NOx sources to NO_3^- in $PM_{2.5}$ were found to be significantly different during a certain sampling period when calculated using different $\delta^{15}N$ data for NOx sources. For instance, during the pre-heating periods, the contributions of soil sources, coal combustion, and biomass burning in Scenario 1 were 23.0 ± 10.1%, 17.8 ± 12.5%, and 24.1 ± 17.3%, respectively. The contributions were slightly lower than the estimated results in Scenario 2 (25.0 ± 7.4%, 19.1 ± 13.2%, and 25.6 ± 18.3%). Furthermore, the contribution of vehicle exhaust exhibited a notable discrepancy, being considerably higher in Scenario 1 (35.1 ± 22.8%) compared to Scenario 2 (30.2 ± 21.1%). Therefore, the calculation of the contributions of various sources to NO_3^- using $\delta^{15}N$ data in NOx sources from previous studies may result in inaccuracies.

The uncertainty index (UI_{90}), derived from posterior distribution data (as detailed in Text S3), serves as a metric to evaluate the uncertainty in the results calculated by the MixSIAR model (Zhang et al., 2024a). A low UI_{90} value indicates a low degree of uncertainty, which suggests that the results of the source contribution were stable (Shang et al., 2020). As shown in Figure 4, the UI_{90} values of coal combustion and biomass combustion were lower in Scenario 1 than in Scenario 2, indicating that the results in Scenario 1 were relatively stable. However, the contributions of vehicle exhaust and soil sources in Scenario 2 were relatively stable, as their UI_{90} values were lower in Scenario 2 than in Scenario 1. It can therefore be observed that the uncertainty in contributions from different sources exhibited a variety of degrees of variability that were influenced by the differing end-member values inputted into the model. Generally, the correlation of probability density functions (PDFs) between different sources may provide insight into the validity of model calculations (Parnell et al., 2010). For instance, if the two sources cannot be completely differentiated by the model, their correlation in PDFs will exhibit a strong negative correlation (Lin et

https://doi.org/10.5194/egusphere-2024-1621
Preprint. Discussion started: 27 June 2024

al., 2021). The study revealed a significant negative correlation between the PDFs of vehicle emissions and coal combustion and soil sources both in both Scenario 1 and Scenario 2 (Table S2), indicating that these sources cannot be completely differentiated. Therefore, the inclusion of additional sources is recommended to enhance the accuracy of estimates provided by the MixSIAR model (Lin et al., 2021).

Since the initiation of the Coal Replacement Project in 2017, the contribution of natural gas combustion to NO_3^- may not be negligible in recent years in Tianjin (Meng et al., 2022;Wang et al., 2022). However, previous studies have seldom examined the role of natural gas combustion in contributing to NO_3^- in $PM_{2.5}$, due to limited availability of reported of $\delta^{15}N$ values of NOx resulting from natural gas combustion (Zong et al., 2022b;Walters et al., 2015b). Consequently, the results may be subject to some degree of uncertainty when only the four $\delta^{15}N$-NOx end-member values are considered. Therefore, we refer to the $\delta^{15}N$-NOx end-member values from natural gas combustion obtained from previous studies (Scenario 3) and locally acquired in Tianjin (Scenario 4) to calculate the relative contribution fractions of the five NOx sources using the MixSIAR model (Figure 4c and 4d).

In contrast to the findings of the four sources (Scenario 1 and Scenario 2), significant discrepancies exist between Scenario 3 and Scenario 4. Especially the contribution fractions of natural gas combustion (21.0 ± 13.8% *vs.* 16.5 ± 11.5%) and coal combustion (18.2 ± 10.7% *vs.* 22.0 ± 12.7%), the results estimated in Scenario 4 significantly differ from those in Scenario 3. These disparities are also present across different sampling periods. During pre-heating periods, contributions of vehicle exhaust (24.9 ± 18.5% *vs.* 25.6 ± 19.0%) and biomass burning (20.9 ± 15.1% *vs.* 24.1 ± 17.2%) were lower in Scenario 4 compared to Scenario 3. Conversely, natural gas combustion (21.5 ± 14.3% *vs.* 17.3 ± 11.3%) and soil sources (14.4 ± 9.7% *vs.* 13.2 ± 8.7%) estimates in Scenario 3 were higher than those in Scenario 4. Similar differences were observed during the mid-heating periods. However, in the late-heating periods, contributions of vehicle exhaust (22.1 ± 18.0% *vs.* 26.0 ± 17.3%) and coal combustion (15.6 ± 10.8% *vs.* 18.2 ± 11.6%) calculated in Scenario 4 was higher than those in Scenario 3. In addition, biomass burning (20.8 ± 14.9% *vs.* 20.6 ± 14.9%), natural gas combustion (24.1 ± 16.1% *vs.* 18.7 ± 13%) and soil sources (17.4 ± 10.8% *vs.* 16.4 ± 9.9%) in Scenario 4 were lower than those in Scenario 3. In both scenarios, the contribution of natural gas combustion to NO_3^- was close to or even exceeds that of soil sources (Figure 4). This underscores the need to consider natural gas combustion when assessing NO_3^- sources in $PM_{2.5}$, particularly in urban areas impacted by the Coal Replacement Project (Zhang et al., 2024a). Consequently, our result further highlight that the natural gas combustion as a source input the model could improve the validity of the calculations to a certain extent. Additionally, measuring the $\delta^{15}N$ values of the local NOx source is necessary to accurately identify the source of NO_3^- in $PM_{2.5}$.

3.4 Industrial emission should be an important source of NO_3^-

Industrial emissions, particularly those from the iron and steel sector, consume a

https://doi.org/10.5194/egusphere-2024-1621
Preprint. Discussion started: 27 June 2024

significant quantity of fossil fuel and mineral resources, resulting in a notable increase in NOx emissions (Wang et al., 2019). The iron and steel industry in China has undergone considerable expansion, resulting in a marked increase in NOx emissions. From 2005 to 2015, emissions escalated from 687.93 kt to 1017.24 kt (Gao et al., 2019). This trend suggests that emissions from this sector increasingly affect urban atmospheric NOx levels, especially in industrial cities. Our investigation has revealed that the δ^{15}N-NOx signature from the iron and steel industry is distinct from that of other sources, such as vehicle exhaust, coal combustion, and natural gas combustion (Figure 1). Consequently, it is necessary to treat this source as a unique end-member in the apportionment of NO_3^-.

The MixSIAR model was used to estimate the contributions of six NOx sources (coal combustion, biomass burning, vehicle exhaust, soil sources, natural gas combustion and industrial emission source) to NO_3^- in $PM_{2.5}$ based on their respective δ^{15}N values. We concluded that coal combustion (22.8 ± 11.9%) was major sources of NO_3^- in $PM_{2.5}$ in Tianjin, followed by the biomass burning (20.9 ± 15.0%) and vehicle exhaust (20.0 ± 17.2%) (Figure S8). In comparison to a previous study in Tianjin (Xiao et al., 2023), where coal combustion contributed 42.6% of NOx, our study observed a significant decrease, attributable to the ultraclean transformation of coal combustion processes. Nevertheless, energy from coal combustion, which remains the main source of NOx in Tianjin, is used for most of the manufacturing and residential sectors. Moreover, there is a possibility that the contribution of coal combustion increased due to long-range transportation of air masses, alongside local emissions (Li et al., 2023). This is particularly significant as there was notable coal combustion activity upwind of Tianjin (Feng et al., 2020;Xiao et al., 2024b). However, the contribution of vehicle exhaust was slightly higher than the results in our earlier study (19.8%) (Xiao et al., 2023), which resulted from the increased of vehicle ownership. It was worth noting that the influence of biomass burning was also decreased than that in earlier study in Tianjin, which attributed to the effective implementation of measures, such as the ban on straw burning in the North China Plain (Huang et al., 2021). In this study, industrial emission source was accounting for 14%, slightly lower than vehicle exhaust. According to the community emission data system, previous studies have estimated the industrial contribution to NOx to be around 14% (Bekker et al., 2023), which close to our estimate result. Moreover, the contribution of the industrial emission source was found to be greater than that of soil sources (10%) and natural gas combustion (12%), indicating that it should be considered an important source of NO_3^-.

Generally, the contribution of certain NOx sources decreased as the number of sources increased (Figure S10). In particular, the contributions from soil and vehicle exhaust sources decreased by 13% and 11%, respectively, compared to the results from four sources. Furthermore, they further decreased by 4% and 4%, respectively, compared to the results from five sources. In this case, however, the contribution of coal combustion was slightly increased (Figure S10). The could indication that the number of sources will markedly influence the estimate results by the MixSIAR

https://doi.org/10.5194/egusphere-2024-1621
Preprint. Discussion started: 27 June 2024

model. Furthermore, the correlations of PDFs between coal combustion and biomass burning remained unchanged, while those between the other sources decreased further when the number of sources input into the model increased from four to six (Table S2). This indicated that the inter-influence between these sources was further reduced, and the model was able to distinguish between them (Lin et al., 2021). Moreover, the contributions of all sources demonstrated more relatively stable results, with UI_{90} values exhibiting the lowest values compared to the results estimated by the four or five sources (Figure 4c) (Zhang et al., 2024a). This is because after setting the total contribution of all sources in the model to 1, the lack of input sources in the model may lead to an increase in the fluctuation of the calculated results (Lin et al., 2021;Zhang et al., 2024a;Feng et al., 2023). Therefore, it was concluded that incorporating industrial sources in MixSIAR model could decrease uncertainty in calculating the contribution of NOx sources.

To further elucidate the reasonable of NO_3^- source apportionment results when the $\delta^{15}N$ signature of NOx from industrial emission sources were input the MixSIAR model, we examine the simulation results of different sampling periods, as shown in Figure 5. It was demonstrated that, irrespective of the sampling period, the contribution of NOx sources varied with the number of sources increased, attributable to the sensitive of MixSIAR model to missing emission sources (Feng et al., 2023). Notably, during the mid-heating periods, coal combustion and biomass burning contributed more significantly than in other periods (Figure 6), collectively exceeding 50% when six sources were incroporated into the MixSIAR model. These findings suggest that winter heating emissions play a dominant role in the increase of NO_3^- concentrations in the urban area of Tianjin (Luo et al., 2019;Zhao et al., 2020). Additionally, the contributions of these two sources were higher during pre-heating compared to late-heating periods, when six sources were considered in the MixSIAR model. These differences were also reflected in the concentrations of trace factor from biomass burning (K^+) and coal combustion (Cl^-) (Sun et al., 2020;Zong et al., 2018) (Figure 6c and 6d). However, the simulation results did not exhibit similar consistency when five or four sources were included in the MixSIAR model. For instance, the contribution of coal combustion was very close in the pre-heating and late-heating periods when five or four sources were considered. Although the contribution of soil sources exhibited similar varied patterns across the three sampling periods when different number of emission sources were considered in the MixSIAR model (Figure 5), the contribution of soil sources estimated with six sources was significantly lower than the results from five or four sources. Especially in the mid-heating period, its contribution was less than 10%. This was expected as low soil temperatures decrease NOx emissions into the atmosphere (Lin et al., 2021). Interestingly, vehicle exhaust was the highest contributor to NOx during the late-heating periods (Figure 5), mainly attributable to the gradual weakening of coal combustion and biomass burning activities for heating as temperatures increase. Although vehicle exhaust emissions of NOx may increase due to the rapid rise in car ownership, their contribution fraction was only around 20%, owing to the three-way catalyst (TWC) and Selective Catalytic Reduction (SCR) equipment installed in petrol

https://doi.org/10.5194/egusphere-2024-1621
Preprint. Discussion started: 27 June 2024

and diesel vehicles to mitigate NOx emissions throughout China (Guan et al., 2014;Gu et al., 2022). It should be noted that the contribution of industrial sources (16.2 ± 12.5%) during the late-heating periods was close to coal combustion (17.7 ± 11.2%), further underscoring the importance of incorporating industrial sources in calculating results using the MixSIAR model. In essence, the exclusion of industrial sources may lead to an increase of more than 15% in the contribution fraction of other sources, biasing source contribution estimates and misguiding emissions reduction measures.

3.5 Limitations and outlook

The dataset presented in this study represents, to the best of our knowledge, the first more systematic attempt to determine the $\delta^{15}N$ values of several significant NOx sources within urban environments in China. However, it is essential to acknowledge that some sources, like bulk coal combustion, the metallurgical industry, and residential gas, were either incompletely sampled or not sampled at all. Additionally, the $\delta^{15}N$ values of NOx emissions from soil across different seasons remain unknown. These omissions could influence the outcomes of source apportionment, and result in several uncertainties. Nevertheless, it can be determined that in the calculation results of the MixSIAR model, the role of local $\delta^{15}N$-NOx source values is critical and should not be overlooked. And as we introduced more sources into the model, the estimates of the contribution of each NOx source grew steadier, and the mutual influence among these sources diminished significantly. This also highlights the importance of comprehensively determining the $\delta^{15}N$ values of typical NOx sources. Therefore, it would be beneficial for NO_3^- source apportionment to further refine the NOx source types and improve the $\delta^{15}N$ values of other NOx sources in the future.

It is widely recognized that different conversion pathways for NOx to NO_3^- exhibit clear isotopic fractionation of nitrogen. This can lead to inaccuracies in estimating the contributions of nitrate sources, particularly because the specific influence of various pathways on the fractionation coefficient εN (NOx → NO_3^-) often remains indistinct (Feng et al., 2020;Zhang et al., 2019). Specialized pathways, such as those involving heterogeneous chlorine chemistry and nitrogen trioxide, can alter the $\delta^{15}N$ values of NO_3^- (Luo et al., 2023;Zhang et al., 2024b). In this study, the $\delta^{18}O$-NO_3^- values helped constrain the fractionation factor from NOx to NO_3^- (Xiao et al., 2020), but only two primary pathways, hydroxyl radical oxidation and nitrogen pentoxide hydrolysis, were taken into account. Previous research supports the view that these pathways account for up to 95% of NO_3^- production (Lin et al., 2021;Xiao et al., 2020), implying that alternative pathways might exert a relatively minor impact on εN calculations. Nonetheless, future measurements of $\Delta^{17}O$- NO_3^- are essential to elucidate the isotopic fractionation coefficients comprehensively during the formation of NO_3^-.

4. Conclusions

In this study, the $\delta^{15}N$ values of 6 NOx sources in the local Tianjin area collected

https://doi.org/10.5194/egusphere-2024-1621
Preprint. Discussion started: 27 June 2024

by the active sampler were determined. Results shown that $\delta^{15}N$ value of NOx emissions from coal combustion exhibited the positive value (+12.3 ± 1.7‰), followed by the biomass burning (+1.2 ± 3.0‰), the vehicle exhaust (-5.2 ± 5.4‰), the industrial emission source (-20.6 ± 16.8‰), the natural gas combustion (-24.8 ± 5.6‰) and the soil sources (-33.7 ± 9.7‰). The observation of significant differences in $\delta^{15}N$-NOx values from disparate sources serves to demonstrate the representative nature of these isotopic fingerprints. Furthermore, the mean values or fluctuation range of $\delta^{15}N$-NOx for almost all sources differed from the values reported abroad in previous studies, suggesting that the $\delta^{15}N$ values of NOx sources has local characteristics.

The contributions of various NOx sources to NO_3^- in $PM_{2.5}$ during sampling periods were estimated based on the MixSIAR model. In result, coal combustion, biomass burning and vehicle exhaust collectively contributed more than 60%, dominating the sources of NO_3^- during sampling periods in Tianjin. However, the relative contribution fraction of each sources shown clear difference when the $\delta^{15}N$-NOx source data from previous studies and this study inputted into the model, respectively. Coal combustion, in particular, has a relative contribution that may be underestimated without considering the localized characteristics of the isotopic fingerprints of NOx source. Remark, as the number of source inputs in the model increases from four to six, the interpretability of the estimated results for the contribution of each source increases. Moreover, the contribution of various NOx sources was becoming more stable, and the inter-influence between various sources was significantly reduced. Specific examples include the values of UI_{90} and PDFs, both of which exhibited a significant downward trend as the number of sources increased. Overall, the refined $\delta^{15}N$ values of NOx sources have been demonstrated to be an effective tool in distinguishing source contributions of NO_3^-, which could help to reduce the uncertainties and inter-influence of each source.

Acknowledgments

This work was supported by the National Natural Science Foundation of China (Grant Nos. 42273020 and 41773006), the Postdoctoral Fellowship Program of China Postdoctoral Science Foundation (Grant No. GZC20231552), the Natural Science Foundation of Tianjin (Grant No. 22JCQNJC00700), the Natural Science Foundation of Henan (222300420128).

Data availability

The datasets used in this study are available at https://doi.org/10.5281/zenodo.11392166 (Xiao et al., 2024c)

Conflict of interest.

The authors declare no conflicts of interest relevant to this study.

https://doi.org/10.5194/egusphere-2024-1621
Preprint. Discussion started: 27 June 2024

Author contributions.

Hao Xiao, Qinkai Li and Xiaodong Li designed the study. Hao Xiao, Qinkai Li, Wenjing Dai and Gaoyang Cui performed field measurements and sample collection; Hao Xiao and Qinkai Li performed chemical analysis; Hao Xiao and Qinkai Li performed data analysis; Hao Xiao wrote the original manuscript; and Shiyuan Ding, and Xiaodong Li reviewed and edited the manuscript.

Reference

Baggs, E. M.: A review of stable isotope techniques for N_2O source partitioning in soils: recent progress, remaining challenges and future considerations, Rapid Commun. Mass Sp., 22, 1664-1672, https://doi.org/10.1002/rcm.3456, 2008.

Bekker, C., Walters, W. W., Murray, L. T., and Hastings, M. G.: Nitrate chemistry in the northeast US – Part 1: Nitrogen isotope seasonality tracks nitrate formation chemistry, Atmos. Chem. Phys., 23, 4185-4201, https://doi.org/10.5194/acp-23-4185-2023, 2023.

Duncan, B. N., Lamsal, L. N., Thompson, A. M., Yoshida, Y., Lu, Z., Streets, D. G., Hurwitz, M. M., and Pickering, K. E.: A space-based, high-resolution view of notable changes in urban NOx pollution around the world (2005–2014), J. Geophys. Res. Atmos., 121, 976-996, https://doi.org/10.1002/2015JD024121, 2016.

Elliott, E. M., Yu, Z., Cole, A. S., and Coughlin, J. G.: Isotopic advances in understanding reactive nitrogen deposition and atmospheric processing, Sci. Tot. Environ., 662, 393-403, https://doi.org/10.1016/j.scitotenv.2018.12.177, 2019.

Fan, M., Zhang, Y., Lin, Y., Cao, F., Zhao, Z., Sun, Y., Qiu, Y., Fu, P., and Wang, Y.: Changes of emission sources to nitrate aerosols in Beijing after the clean air actions: evidence from dual isotope compositions, J. Geophys. Res. Atmos., 125, 1-15, https://doi.org/10.1029/2019JD031998, 2020.

Felix, J. D., Elliott, E. M., and Shaw, S. L.: Nitrogen isotopic composition of coal-fired power plant NO_x: influence of emission controls and implications for global emission inventories, Environ. Sci. Technol., 46, 3528-3535, https://doi.org/10.1021/es203355v, 2012.

Felix, J. D., and Elliott, E. M.: The agricultural history of human-nitrogen interactions as recorded in ice core $\delta^{15}N\text{-}NO_3^-$, Geophys. Res. Lett., 40, 1642-1646, https://doi.org/10.1002/grl.50209, 2013.

Felix, J. D., and Elliott, E. M.: Isotopic composition of passively collected nitrogen dioxide emissions: Vehicle, soil and livestock source signatures, Atmos. Environ., 92, 359-366, https://doi.org/10.1016/j.atmosenv.2014.04.005, 2014.

Feng, X., Li, Q., Tao, Y., Ding, S., Chen, Y., and Li, X.: Impact of coal replacing Project on atmospheric fine aerosol nitrate loading and formation pathways in urban Tianjin: Insights from chemical composition and ^{15}N and ^{18}O isotope ratios, Sci. Tot. Environ., 708, 134797, https://doi.org/10.1016/j.scitotenv.2019.134797, 2020.

Feng, X., Chen, Y., Du, H., Feng, Y., Mu, Y., and Chen, J.: Biomass burning is a non-negligible source for ammonium during winter haze episodes in rural North China: Evidence from high time resolution ^{15}N-stable isotope, J. Geophys. Res. Atmos., 128, e2022JD038012, https://doi.org/10.1029/2022JD038012, 2023.

Fibiger, D. L., Hastings, M. G., Lew, A. F., and Peltier, R. E.: Collection of NO and NO_2 for Isotopic Analysis of NO_x Emissions, Anal. Chem., 86, 12115-12121, https://doi.org/10.1021/ac502968e,

https://doi.org/10.5194/egusphere-2024-1621
Preprint. Discussion started: 27 June 2024

2014.

Fibiger, D. L., and Hastings, M. G.: First measurements of the nitrogen isotopic composition of NOx from biomass burning, Environ. Sci. Technol. , 50, 11569-11574, https://doi.org/10.1021/acs.est.6b03510, 2016.

Gao, C., Gao, W., Song, K., Na, H., Tian, F., and Zhang, S.: Spatial and temporal dynamics of air-pollutant emission inventory of steel industry in China: A bottom-up approach, Resour. Conserv. Recy., 143, 184-200, https://doi.org/10.1016/j.resconrec.2018.12.032, 2019.

Gao, J., Wei, Y., Shi, G., Yu, H., Zhang, Z., Song, S., Wang, W., Liang, D., and Feng, Y.: Roles of RH, aerosol pH and sources in concentrations of secondary inorganic aerosols, during different pollution periods, Atmos. Environ., 241, 117770, https://doi.org/10.1016/j.atmosenv.2020.117770, 2020.

Gu, M., Pan, Y., Walters, W. W., Sun, Q., Song, L., Wang, Y., Xue, Y., and Fang, Y.: Vehicular emissions enhanced ammonia concentrations in winter mornings: Insights from diurnal nitrogen isotopic signatures, Environ. Sci. Technol., 56, 1578-1585, https://doi.org/10.1021/acs.est.1c05884, 2022.

Guan, B., Zhan, R., Lin, H., and Huang, Z.: Review of state of the art technologies of selective catalytic reduction of NOx from diesel engine exhaust, Appl. Therm. Eng., 66, 395-414, https://doi.org/10.1016/j.applthermaleng.2014.02.021, 2014.

Guo, W., Luo, L., Zhang, Z., Zheng, N., Xiao, H., and Xiao, H.: The use of stable oxygen and nitrogen isotopic signatures to reveal variations in the nitrate formation pathways and sources in different seasons and regions in China, Environ. Res., 201, 111537, https://doi.org/10.1016/j.envres.2021.111537, 2021.

Hall, S. J., Matson, P. A., and Roth, P. M.: NOx emissions from soil: Implications for air quality modeling in agricultural regions, Annu. Rev. Env. Resour., 21, 311-346, https://doi.org/10.1146/annurev.energy.21.1.311, 1996.

Hastings, M. G., Jarvis, J. C., and Steig, E. J.: Anthropogenic impacts on nitrogen isotopes of ice-core nitrate, Science, 324, 1288-1288, https://doi.org/10.1126/science.1170510, 2009.

Hayhurst, A. N., and Vince, I. M.: Nitric oxide formation from N2 in flames: The importance of "prompt" NO, Prog. Energ. Combust., 6, 35-51, https://doi.org/10.1016/0360-1285(80)90014-3, 1980.

Heaton, T. H. E.: $^{15}N/^{14}N$ ratios of NO_x from vehicle engines and coal-fired power stations, Tellus, 42, 304-307, https://doi.org/10.1034/j.1600-0889.1990.00007.x-i1, 1990.

Huang, L., Zhu, Y., Wang, Q., Zhu, A., Liu, Z., Wang, Y., Allen, D. T., and Li, L.: Assessment of the effects of straw burning bans in China: Emissions, air quality, and health impacts, Sci. Tot. Environ., 789, 147935, https://doi.org/10.1016/j.scitotenv.2021.147935, 2021.

Huang, R., Zhang, Y., Bozzetti, C., Ho, K., Cao, J., Han, Y., Daellenbach, K. R., Slowik, J. G., Platt, S. M., Canonaco, F., Zotter, P., Wolf, R., Pieber, S. M., Bruns, E. A., Crippa, M., Ciarelli, G., Piazzalunga, A., Schwikowski, M., Abbaszade, G., Schnelle-Kreis, J., Zimmermann, R., An, Z., Szidat, S., Baltensperger, U., Haddad, I. E., and Prévôt, A. S. H.: High secondary aerosol contribution to particulate pollution during haze events in China, Nature, 514, 218-222, https://doi.org/10.1038/nature13774, 2014.

Huang, T., Zhu, X., Zhong, Q., Yun, X., Meng, W., Li, B., Ma, J., Zeng, E. Y., and Tao, S.: Spatial and temporal trends in global emissions of nitrogen oxides from 1960 to 2014, Environ. Sci. Technol., 51, 7992-8000, https://doi.org/10.1021/acs.est.7b02235, 2017.

https://doi.org/10.5194/egusphere-2024-1621
Preprint. Discussion started: 27 June 2024

Li, D., and Wang, X.: Nitrogen isotopic signature of soil-released nitric oxide (NO) after fertilizer application, Atmos. Environ., 42, 4747-4754, https://doi.org/10.1016/j.atmosenv.2008.01.042, 2008.

Li, Q., Li, X., Yang, Z., Cui, G., and Ding, S.: Diurnal and seasonal variations in water-soluble inorganic ions and nitrate dual isotopes of $PM_{2.5}$: Implications for source apportionment and formation processes of urban aerosol nitrate, Atmos. Res., 248, 105197, https://doi.org/10.1016/j.atmosres.2020.105197, 2021.

Li, T., Li, J., Sun, Z., Jiang, H., Tian, C., and Zhang, G.: High contribution of anthropogenic combustion sources to atmospheric inorganic reactive nitrogen in South China evidenced by isotopes, Atmos. Chem. Phys., 23, 6395-6407, https://doi.org/10.5194/acp-23-6395-2023, 2023.

Lin, Y.-C., Zhang, Y.-L., Yu, M., Fan, M.-Y., Xie, F., Zhang, W.-Q., Wu, G., Cong, Z., and Michalski, G.: Formation mechanisms and source apportionments of airborne nitrate aerosols at a Himalayan-Tibetan Plateau site: Insights from nitrogen and oxygen isotopic compositions, Environ. Sci. Technol., 55, 12261-12271, https://doi.org/10.1021/acs.est.1c03957, 2021.

Luo, L., Wu, Y., Xiao, H., Zhang, R., Lin, H., Zhang, X., and Kao, S.: Origins of aerosol nitrate in Beijing during late winter through spring, Sci. Tot. Environ., 653, 776-782, https://doi.org/10.1016/j.scitotenv.2018.10.306, 2019.

Luo, L., Pan, Y., Zhu, R., Zhang, Z., Zheng, N., Liu, Y., Liu, C., Xiao, H., and Xiao, H.: Assessment of the seasonal cycle of nitrate in $PM_{2.5}$ using chemical compositions and stable nitrogen and oxygen isotopes at Nanchang, China, Atmos. Environ., 225, 117371, https://doi.org/10.1016/j.atmosenv.2020.117371, 2020a.

Luo, L., Zhu, R. G., Song, C. B., Peng, J. F., and Xiao, H. Y.: Changes in nitrate accumulation mechanisms as $PM_{2.5}$ levels increase on the North China Plain: A perspective from the dual isotopic compositions of nitrate, Chemosphere, 263, 127915, https://doi.org/10.1016/j.chemosphere.2020.127915, 2020b.

Luo, L., Wu, S., Zhang, R., Wu, Y., Li, J., and Kao, S.-j.: What controls aerosol $\delta^{15}N\text{-}NO_3^-$? NOx emission sources vs. nitrogen isotope fractionation, Sci. Tot. Environ., 871, 162185, https://doi.org/10.1016/j.scitotenv.2023.162185, 2023.

Meng, F., Zhang, Y., Kang, J., Heal, M. R., Reis, S., Wang, M., Liu, L., Wang, K., Yu, S., Li, P., Wei, J., Hou, Y., Zhang, Y., Liu, X., Cui, Z., Xu, W., and Zhang, F.: Trends in secondary inorganic aerosol pollution in China and its responses to emission controls of precursors in wintertime, Atmos. Chem. Phys., 22, 6291-6308, https://doi.org/10.5194/acp-22-6291-2022, 2022.

Meng, X., Wu, Z., Chen, J., Qiu, Y., Zong, T., Song, M., Lee, J., and Hu, M.: Particle phase state and aerosol liquid water greatly impact secondary aerosol formation: insights into phase transition and its role in haze events, Atmos. Chem. Phys., 24, 2399-2414, https://doi.org/10.5194/acp-24-2399-2024, 2024.

Parnell, A. C., Inger, R., Bearhop, S., and Jackson, A. L.: Source partitioning using stable isotopes: Coping with too much variation, PLOS ONE, 5, e9672, https://doi.org/10.1371/journal.pone.0009672, 2010.

Sada, E., Kumazawa, H., Hayakawa, N., Kudo, I., and Kondo, T.: Absorption of NO in aqueous solutions of $KMnO_4$, Chem. Eng. Sci., 32, 1171-1175, https://doi.org/10.1016/0009-2509(77)80049-3, 1977.

Shang, X., Huang, H., Mei, K., Xia, F., Chen, Z., Yang, Y., Dahlgren, R. A., Zhang, M., and Ji, X.: Riverine nitrate source apportionment using dual stable isotopes in a drinking water source

https://doi.org/10.5194/egusphere-2024-1621
Preprint. Discussion started: 27 June 2024

watershed of southeast China, Sci. Tot. Environ., 724, 137975, https://doi.org/10.1016/j.scitotenv.2020.137975, 2020.

Shi, Y., Tian, P., Jin, Z., Hu, Y., Zhang, Y., and Li, F.: Stable nitrogen isotope composition of NOx of biomass burning in China, Sci. Tot. Environ., 803, 149857, https://doi.org/10.1016/j.scitotenv.2021.149857, 2022.

Song, W., Wang, Y., Yang, W., Sun, X., Tong, Y., Wang, X., Liu, C., Bai, Z., and Liu, X.: Isotopic evaluation on relative contributions of major NOx sources to nitrate of $PM_{2.5}$ in Beijing, Environ. Pollut., 248, 183-190, https://doi.org/10.1016/j.envpol.2019.01.081, 2019.

Song, W., Liu, X.-Y., Hu, C.-C., Chen, G.-Y., Liu, X.-J., Walters, W. W., Michalski, G., and Liu, C.-Q.: Important contributions of non-fossil fuel nitrogen oxides emissions, Nat. Commun., 12, 243, https://doi.org/10.1038/s41467-020-20356-0, 2021.

Sun, X., Zong, Z., Wang, K., Li, B., Fu, D., Shi, X., Tang, B., Lu, L., Thapa, S., Qi, H., and Tian, C.: The importance of coal combustion and heterogeneous reaction for atmospheric nitrate pollution in a cold metropolis in China: Insights from isotope fractionation and Bayesian mixing model, Atmos. Environ., 243, 117730, https://doi.org/10.1016/j.atmosenv.2020.117730, 2020.

Toof, J. L.: A model for the prediction of thermal, prompt, and fuel NOx emissions from combustion turbines, J. Eng. Gas Turbines Power., 108, 340-347, https://doi.org/10.1115/1.3239909, 1986.

Walters, W. W., Goodwin, S. R., and Michalski, G.: Nitrogen stable isotope composition ($\delta^{15}N$) of vehicle-emitted NO_x, Environ. Sci. Technol., 49, 2278-2285, https://doi.org/10.1021/es505580v, 2015a.

Walters, W. W., Tharp, B. D., Fang, H., Kozak, B. J., and Michalski, G.: Nitrogen isotope composition of thermally produced NOx from various fossil-fuel combustion sources, Environ. Sci. Technol., 49, 11363-11371, https://doi.org/10.1021/acs.est.5b02769, 2015b.

Walters, W. W., Fang, H., and Michalski, G.: Summertime diurnal variations in the isotopic composition of atmospheric nitrogen dioxide at a small midwestern United States city, Atmos. Environ., 179, 1-11, https://doi.org/10.1016/j.atmosenv.2018.01.047, 2018.

Wang, J., Gao, J., Che, F., Wang, Y., Lin, P., and Zhang, Y.: Decade-long trends in chemical component properties of $PM_{2.5}$ in Beijing, China (2011−2020), Sci. Tot. Environ., 832, 154664, https://doi.org/10.1016/j.scitotenv.2022.154664, 2022.

Wang, X., Lei, Y., Yan, L., Liu, T., Zhang, Q., and He, K.: A unit-based emission inventory of SO_2, NOx and PM for the Chinese iron and steel industry from 2010 to 2015, Sci. Tot. Environ., 676, 18-30, https://doi.org/10.1016/j.scitotenv.2019.04.241, 2019.

Williams, L. B., Ferrell, R. E., Hutcheon, I., Bakel, A. J., Walsh, M. M., and Krouse, H. R.: Nitrogen isotope geochemistry of organic matter and minerals during diagenesis and hydrocarbon migration, Geochim. Cosmochim. Ac., 59, 765-779, https://doi.org/10.1016/0016-7037(95)00005-K, 1995.

Xiao, H., Ding, S. Y., Ji, C. W., Li, Q. K., and Li, X. D.: Combustion related ammonia promotes $PM_{2.5}$ accumulation in autumn in Tianjin, China, Atmos. Res., 275, 106225, https://doi.org/10.1016/j.atmosres.2022.106225, 2022.

Xiao, H., Ding, S. Y., Ji, C. W., Li, Q. K., and Li, X. D.: Strict control of biomass burning inhibited particulate matter nitrate pollution over Tianjin: Perspective from dual isotopes of nitrate, Atmos. Environ., 293, 119460, https://doi.org/10.1016/j.atmosenv.2022.119460, 2023.

Xiao, H., Ding, S., and Li, X.: Sources of NH_4^+ in $PM_{2.5}$ and their seasonal variations in urban Tianjin China: New insights from the seasonal $\delta^{15}N$ values of NH_3 source, J. Geophys. Res. Atmos., 129, e2023JD040169, https://doi.org/10.1029/2023JD040169, 2024a.

https://doi.org/10.5194/egusphere-2024-1621
Preprint. Discussion started: 27 June 2024

Xiao, H., Ji, C., Ding, S., and Li, X.: Strategic control of combustion-induced ammonia emissions: A key initiative for substantial $PM_{2.5}$ reduction in Tianjin, North China Plain, Sci. Tot. Environ., 928, 172328, https://doi.org/10.1016/j.scitotenv.2024.172328, 2024b.

Xiao, H., Li, Q., Ding, S., Dai, W., and Li, X.: Technical note: Refining $\delta^{15}N$ isotopic fingerprints of local NOx for accurate source identification of nitrate in $PM_{2.5}$ [Dataset], Zenodo, https://doi.org/10.5281/zenodo.11392166, 2024c.

Xiao, H. W., Zhu, R. G., Pan, Y. Y., Guo, W., Zheng, N. J., Liu, Y. H., Liu, C., Zhang, Z. Y., Wu, J. F., Kang, C. A., Luo, L., and Xiao, H. Y.: Differentiation between nitrate aerosol formation pathways in a Southeast Chinese city by dual isotope and modeling studies, J. Geophys. Res. Atmos., 125, e2020JD032604, https://doi.org/10.1029/2020jd032604, 2020.

Xie, Y., Wang, G., Wang, X., Chen, J., and Gao, J.: Nitrate-dominated $PM_{2.5}$ and elevation of particle pH observed in urban Beijing during the winter of 2017, Atmos. Chem. Phys., 20, 5019–5033, https://doi.org/10.5194/acp-20-5019-2020, 2019.

Yu, Z., and Elliott, E. M.: Novel method for nitrogen isotopic analysis of soil-emitted nitric oxide, Environ. Sci. Technol., 51, 6268-6278, https://doi.org/10.1021/acs.est.7b00592, 2017.

Zhang, W., Bi, X., Zhang, Y., Wu, J., and Feng, Y.: Diesel vehicle emission accounts for the dominate NOx source to atmospheric particulate nitrate in a coastal city: Insights from nitrate dual isotopes of $PM_{2.5}$, Atmos. Res., 278, 106328, https://doi.org/10.1016/j.atmosres.2022.106328, 2022.

Zhang, W., Wu, F., Luo, X., Song, L., Wang, X., Zhang, Y., Wu, J., Xiao, Z., Cao, F., Bi, X., and Feng, Y.: Quantification of NOx sources contribution to ambient nitrate aerosol, uncertainty analysis and sensitivity analysis in a megacity, Sci. Tot. Environ., 926, 171583, https://doi.org/10.1016/j.scitotenv.2024.171583, 2024a.

Zhang, Y., Tian, J., Wang, Q., Qi, L., Manousakas, M. I., Han, Y., Ran, W., Sun, Y., Liu, H., Zhang, R., Wu, Y., Cui, T., Daellenbach, K. R., Slowik, J. G., Prévôt, A. S. H., and Cao, J.: High-time-resolution chemical composition and source apportionment of $PM_{2.5}$ in northern Chinese cities: implications for policy, Atmos. Chem. Phys., 23, 9455-9471, https://doi.org/10.5194/acp-23-9455-2023, 2023.

Zhang, Z., Zheng, N., Zhang, D., Xiao, H., and Xiao, H.: Rayleigh based concept to track NO_x emission sources in urban areas of China, Sci. Tot. Environ., 704, 135362, https://doi.org/10.1016/j.scitotenv.2019.135362, 2019.

Zhang, Z., Guan, H., Luo, L., Zheng, N., Xiao, H., Liang, Y., and Xiao, H.: Sources and transformation of nitrate aerosol in winter 2017–2018 of megacity Beijing: Insights from an alternative approach, Atmos. Environ., 241, 117842, https://doi.org/10.1016/j.atmosenv.2020.117842, 2020.

Zhang, Z., Tian, C., Liang, Y., and Zheng, N.: Recent isotopic evidence for elevated vehicular NO_x emission to atmospheric nitrate formation in Chinese megacities, ACS Earth Spac. Chem., 5, 2372-2379, https://doi.org/10.1021/acsearthspacechem.1c00166, 2021.

Zhang, Z., Jiang, Z., Zhou, T., and Geng, L.: Reconciling modeled and observed $\Delta^{17}O(NO_3^-)$ in Beijing winter haze with heterogeneous chlorine chemistry, J. Geophys. Res. Atmos., 129, e2023JD039740, https://doi.org/10.1029/2023JD039740, 2024b.

Zhao, Y., Zhou, Y., Qiu, L., and Zhang, J.: Quantifying the uncertainties of China's emission inventory for industrial sources: From national to provincial and city scales, Atmos. Environ., 165, 207-221, https://doi.org/10.1016/j.atmosenv.2017.06.045, 2017.

Zhao, Z., Cao, F., Fan, M., Zhang, W., Zhai, X., Wang, Q., and Zhang, Y.: Coal and biomass burning as major emissions of NO_x in Northeast China: Implication from dual isotopes analysis of fine nitrate

https://doi.org/10.5194/egusphere-2024-1621
Preprint. Discussion started: 27 June 2024

aerosols, Atmos. Environ., 242, 117762, https://doi.org/10.1016/j.atmosenv.2020.117762, 2020.

Zhao, Z. Y., Cao, F., Fan, M. Y., Zhai, X. Y., Yu, H. R., Hong, Y., Ma, Y. J., and Zhang, Y. L.: Nitrate aerosol formation and source assessment in winter at different regions in Northeast China, Atmos. Environ., 267, 118767, https://doi.org/10.1016/j.atmosenv.2021.118767, 2021.

Zong, Z., Wang, X., Tian, C., Chen, Y., Fang, Y., Zhang, F., Li, C., Sun, J., Li, J., and Zhang, G.: First assessment of NO_x sources at a regional background site in North China using isotopic analysis linked with modeling, Environ. Sci. Technol., 51, 5923-5931, https://doi.org/10.1021/acs.est.6b06316, 2017.

Zong, Z., Tan, Y., Wang, X., Tian, C., Fang, Y., Chen, Y., Fang, Y., Han, G., Li, J., and Zhang, G.: Assessment and quantification of NO_x sources at a regional background site in North China: Comparative results from a Bayesian isotopic mixing model and a positive matrix factorization model, Environ. Pollut., 242, 1379-1386, https://doi.org/10.1016/j.envpol.2018.08.026, 2018.

Zong, Z., Sun, Z., Xiao, L., Tian, C., Liu, J., Sha, Q., Li, J., Fang, Y., Zheng, J., and Zhang, G.: Insight into the variability of the nitrogen isotope composition of vehicular NOx in China, Environ. Sci. Technol., 54, 14246-14253, https://doi.org/10.1021/acs.est.0c04749, 2020a.

Zong, Z., Tan, Y., Wang, X., Tian, C., Li, J., Fang, Y., Chen, Y., Cui, S., and Zhang, G.: Dual-modelling-based source apportionment of NO_x in five Chinese megacities: Providing the isotopic footprint from 2013 to 2014, Environ. Int., 137, 105592, https://doi.org/10.1016/j.envint.2020.105592, 2020b.

Zong, Z., Shi, X., Sun, Z., Tian, C., Li, J., Fang, Y., Gao, H., and Zhang, G.: Nitrogen isotopic composition of NOx from residential biomass burning and coal combustion in North China, Environ. Pollut., 304, 119238, https://doi.org/10.1016/j.envpol.2022.119238, 2022a.

Zong, Z., Tian, C., Sun, Z., Tan, Y., Shi, Y., Liu, X., Li, J., Fang, Y., Chen, Y., Ma, Y., Gao, H., Zhang, G., and Wang, T.: Long-term evolution of particulate nitrate pollution in North China: Isotopic evidence from 10 offshore cruises in the Bohai Sea from 2014 to 2019, J. Geophys. Res. Atmos., e2022JD036567, https://doi.org/10.1029/2022JD036567, 2022b.

Zou, J., Liu, Z., Hu, B., Huang, X., Wen, T., Ji, D., Liu, J., Yang, Y., Yao, Q., and Wang, Y.: Aerosol chemical compositions in the North China Plain and the impact on the visibility in Beijing and Tianjin, Atmos. Res., 201, 235-246, https://doi.org/10.1016/j.atmosres.2017.09.014, 2018.

https://doi.org/10.5194/egusphere-2024-1621
Preprint. Discussion started: 27 June 2024

Table 1 Comparison of the $\delta^{15}N$ characteristic spectra of NO_x sources reported in the previous and present study

NO_x sources	Previous studies				This study		
	av (‰)	std (‰)	n	Reference	av (‰)	std (‰)	n
Coal combustion	+13.7	4.6	47	(Walters et al., 2015b;Felix et al., 2012)	+12.3	1.7	13
Vehicle exhaust	−7.2	7.8	151	(Walters et al., 2015b;Walters et al., 2015a;Felix and Elliott, 2014;Heaton, 1990)	−5.2	5.4	62
Biomass burning	+1.0	4.1	24	(Fibiger and Hastings, 2016;Felix and Elliott, 2013;Hastings et al., 2009)	+1.2	3.0	14
Soil emission	−33.8	12.2	6	(Felix and Elliott, 2014;Li and Wang, 2008)	−33.7	9.7	12
Nature gas combustion	−16.5	1.7	23	(Walters et al., 2015b)	−24.8	5.6	5
Industrial source	N/A	N/A		N/A	−20.6	16.8	17

Note：N/A represents data unknown.

https://doi.org/10.5194/egusphere-2024-1621
Preprint. Discussion started: 27 June 2024

875 Table 2 Mean mass concentrations of $PM_{2.5}$ and water-soluble inorganic ions as well as the $\delta^{15}N$-
876 NO_3^- in Tianjin urban areas at different sampling stages for 2018 ~ 2019 (av ± std)

Species	All days Average (n = 142)	Pre-heating Average (n = 56)	Mid-heating Average (n = 30)	Late-heating Average (n = 56)
$PM_{2.5}$ (μg m^{-3})	68.6 ± 62.4	75.3 ± 53.3	68.9 ± 43.2	39.0 ± 27.9
SO_4^{2-} (μg m^{-3})	4.9 ± 4.2	5.9 ± 4.2	6.1 ± 6.0	3.1 ± 1.9
NO_3^- (μg m^{-3})	12.7 ± 10.8	16.0 ± 12.4	11.9 ± 9.4	9.7 ± 8.7
NH_4^+ (μg m^{-3})	7.7 ± 7.2	10.4 ± 9.0	7.9 ± 6.0	4.8 ± 4.0
Cl^- (μg m^{-3})	2.3 ± 2.1	2.7 ± 2.0	4.0 ± 2.5	0.9 ± 8.4
K^+ (μg m^{-3})	0.7 ± 0.6	0.8 ± 0.7	0.9 ± 0.5	0.4 ± 0.3
Ca^{2+} (μg m^{-3})	0.2 ± 0.1	0.1 ± 0.1	0.1 ± 0.1	0.2 ± 0.1
Na^+ (μg m^{-3})	0.2 ± 0.1	0.2 ± 0.1	0.3 ± 0.1	0.2 ± 0.1
Mg^{2+} (μg m^{-3})	0.01 ± 0.03	0.03 ± 0.02	0.03 ± 0.01	0.03 ± 0.02
$\delta^{15}N$ (‰)	8.5 ± 4.4	7.7 ± 4.1	12.4 ± 3.3	7.1 ± 4.1

https://doi.org/10.5194/egusphere-2024-1621
Preprint. Discussion started: 27 June 2024

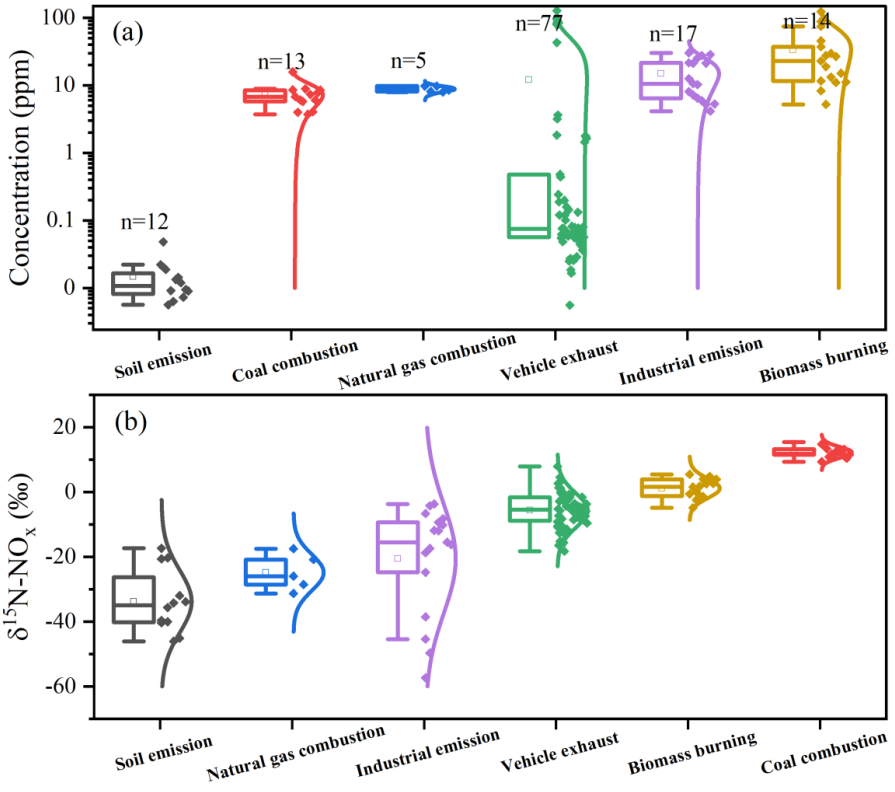

Figure 1 Concentration (a) and (b) $\delta^{15}N$ value of NOx in each emission sources. The box-whisker plot symbols represent the 25th–75th percentiles. The curved lines to the right of the box-whisker plot symbols illustrate the probability distribution of the sample points, each of which represents one sample.

https://doi.org/10.5194/egusphere-2024-1621
Preprint. Discussion started: 27 June 2024

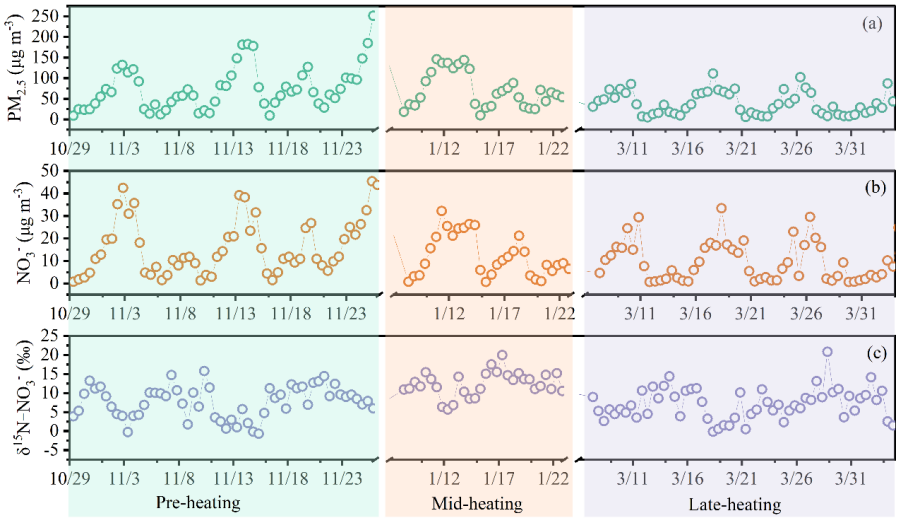

Figure 2 Time series of the concentrations in $PM_{2.5}$ (a) and NO_3^- (b), as well as the $\delta^{15}N$ values (c) in NO_3^-.

https://doi.org/10.5194/egusphere-2024-1621
Preprint. Discussion started: 27 June 2024

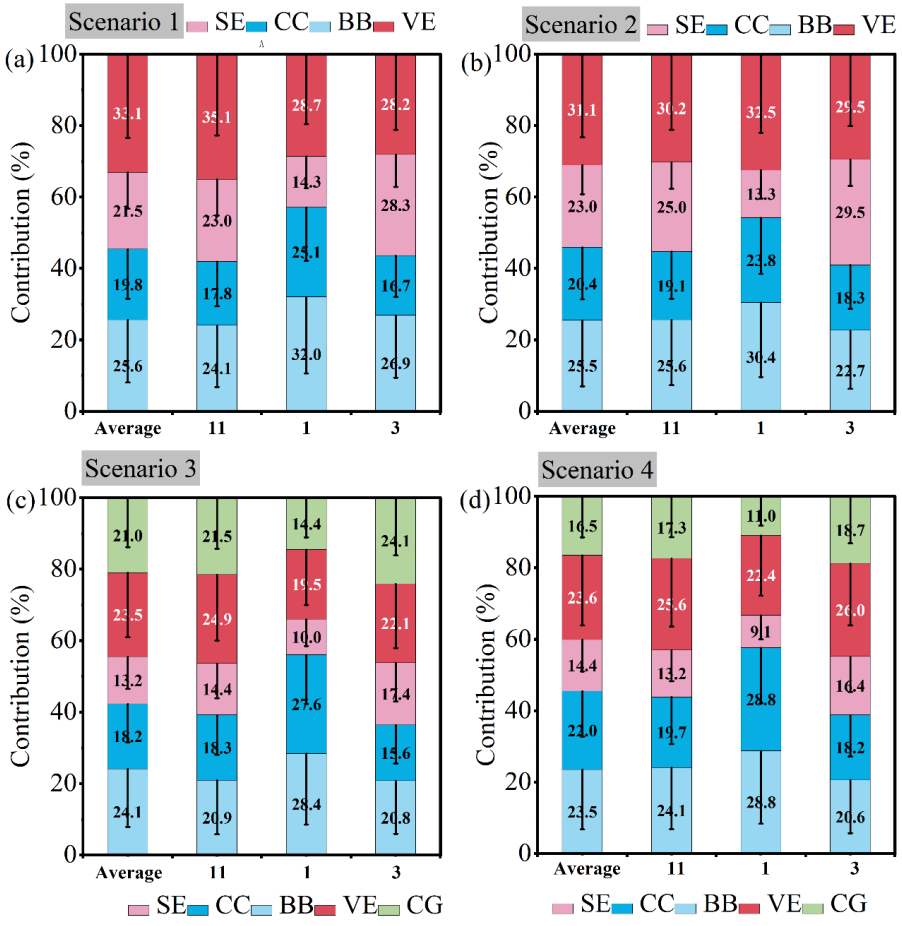

Figure 3 Comparison of fractional contributions of NO_3^- sources in $PM_{2.5}$ in Tianjin estimated by different $\delta^{15}N$ values of NOx sources. The results of Scenario 1 and Scenario 3 were estimated using the $\delta^{15}N$ values of four and five NOx sources obtained from previous studies, while the results of Scenario 1 and Scenario 3 were estimated using the $\delta^{15}N$ values of four and five NOx sources obtained from this study. Also, SE = soil emission, CC = coal combustion, BB = biomass burning, VE = vehicle emission, and CG = combustion of natural gas.

https://doi.org/10.5194/egusphere-2024-1621
Preprint. Discussion started: 27 June 2024

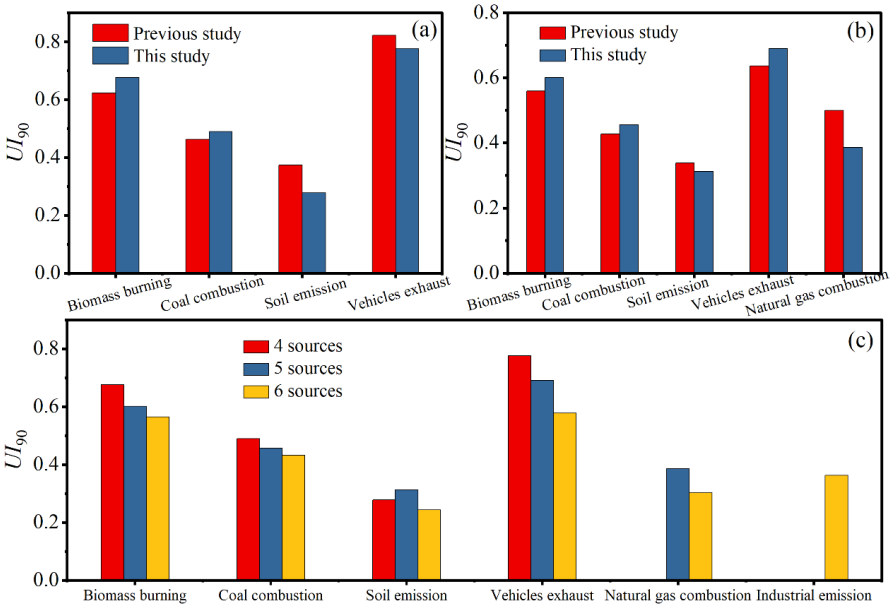

Figure 4 (a) The UI_{90} values of the contribution fraction of the four sources estimated by the isotopic fingerprint in NOx sources obtained from previous studies and this study. (b) The UI_{90} values of the contribution fraction of the five sources estimated by the isotopic fingerprint in NOx sources obtained from previous studies and this study. (c) The UI_{90} values of the contribution fraction of the four, five, and six sources estimated by the isotopic fingerprint in NOx sources obtained from this study.

https://doi.org/10.5194/egusphere-2024-1621
Preprint. Discussion started: 27 June 2024

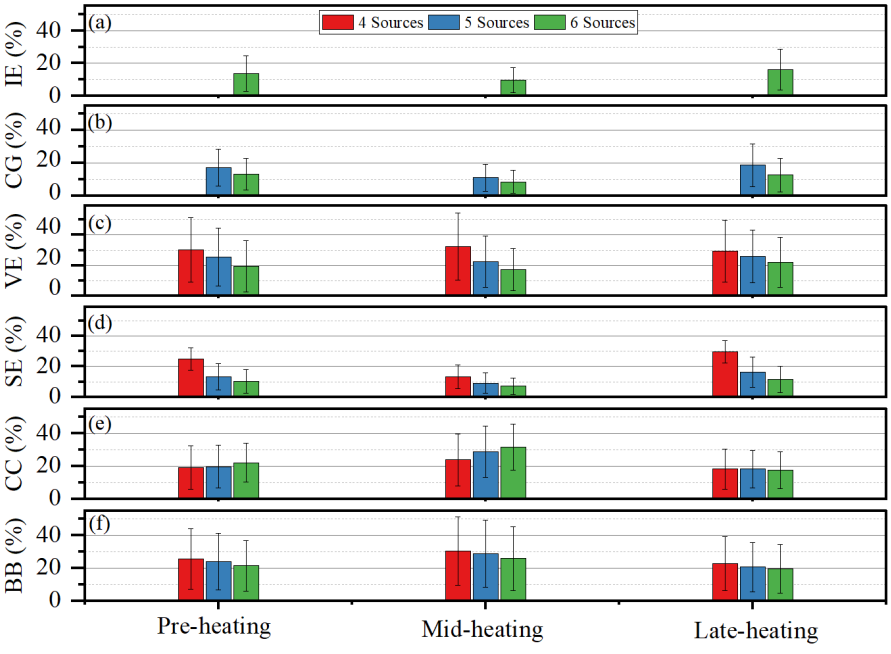

Figure 5 The contribution fraction of the four, five, and six sources in different periods estimated by the isotopic fingerprint in NOx sources obtained from this study. Also, SE = soil emission, CC = coal combustion, BB = biomass burning, VE = vehicle emission, and CG = combustion of natural gas.

https://doi.org/10.5194/egusphere-2024-1621
Preprint. Discussion started: 27 June 2024

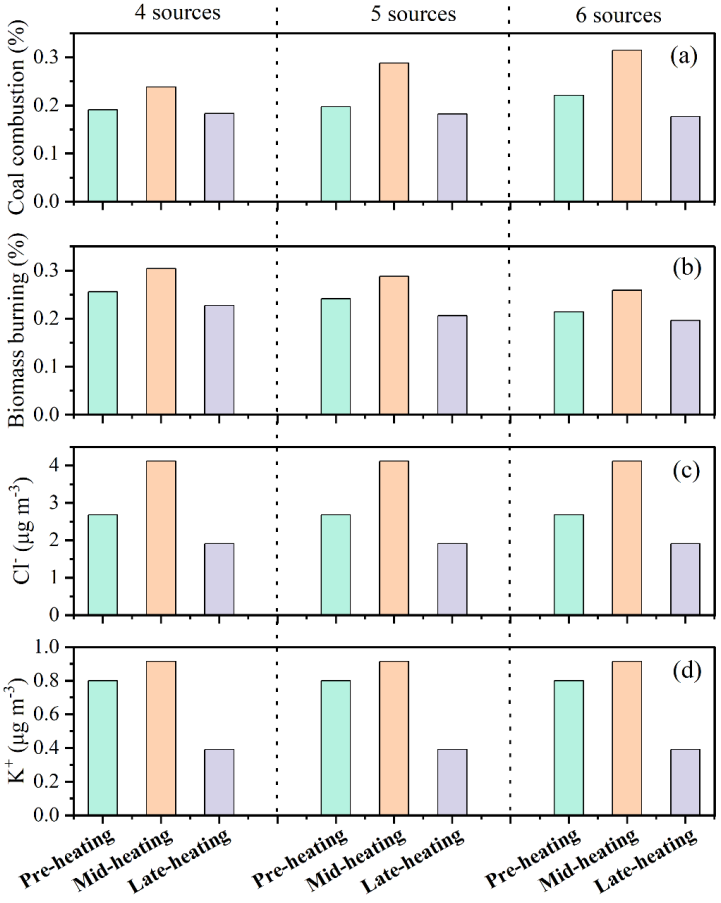

Figure 6 The version trend in contribution fractions of coal combustion (a) and biomass burning (b) in different periods estimated by the isotopic fingerprint in NOx sources of four, five and six sources obtained from this study. (c) and (d) were the version trend in concentrations of Cl^- and K^+ during different sampling periods.

https://doi.org/10.5194/egusphere-2024-1621
Preprint. Discussion started: 27 June 2024

Graphical Abstract